

Impedance Based Characterization of Raw Materials Used in Electrochemical Manufacturing

by Douglas P. Riemer and Mark E. Orazem

Manufacturing of precision stainless steel parts by electrochemical methods such as through-mask etching allow for nearly arbitrary shapes and sizes. An example of such precision components include micro-surgical blades where the blade shape and edge are both created in the electrochemical process, (Fig. 1a and c). Surgical blade edges made using this process require no post-manufacturing sharpening process and hold their edge longer than ground blades due to the electrochemical process enabling the steel temper to be properly maintained.

Another example is the manufacture of hard disk drive suspension assemblies, where the shape of the stainless steel component is produced by the same etching techniques. Here, modifications to the mass and spring properties in the hard disk suspension assembly can also be made by partially etching away some of the material (Fig. 1b).

Through-mask etching allows many components to be made in parallel, greatly reducing costs at high volume, and holding dimensional tolerances to that of the photolithography capability, material thickness, and the fluid mechanics of the etching process. This is often an order of magnitude better than what can be accomplished by mechanical machining.

Many of the electrochemical processes used to make advanced components are sensitive to the state of the oxide film on the raw materials used in the manufacturing process. Photo-resist adhesion, etch initiation, and laser welding are examples that would affect product performance and quality. High yield manufacturing requires raw materials (precursors) with consistent surface properties to obtain repeatable results. To be able to understand the extent to which the oxide state (on the surface of the precursor) influences process parameters, appropriate measurement methods are required to probe the relevant properties that would change with oxide coverage. Electrochemical impedance spectroscopy (EIS) and X-ray photoelectron spectroscopy (XPS) are excellent methods for this purpose. This article outlines a case study wherein these techniques have been employed to probe the growth of oxide films on a stainless steel sample that represented the precursor, and provides a practical example of how such methods can be beneficially used in practice during electrochemical manufacturing processes.

(continued on next page)

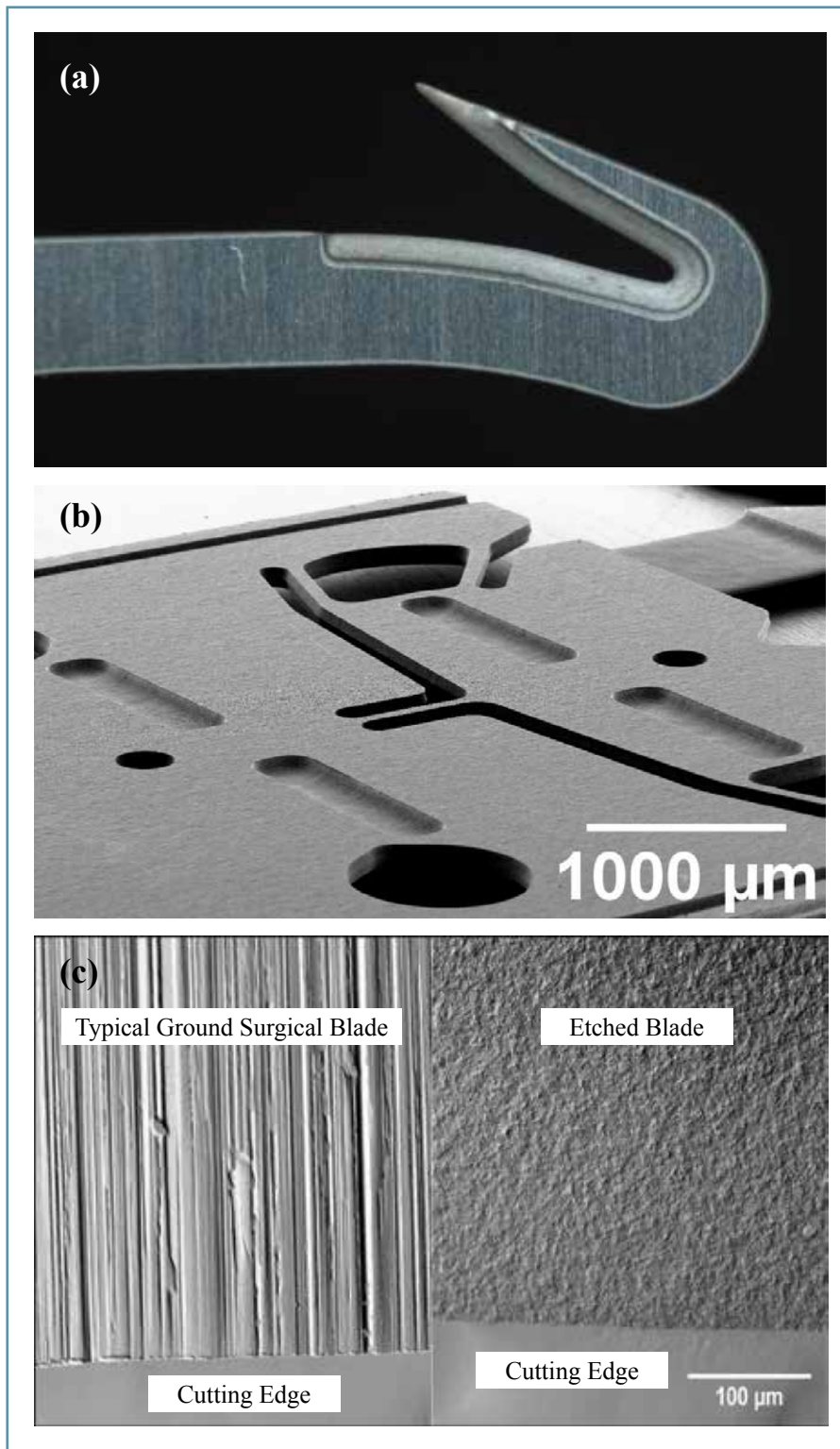


FIG. 1. Examples of through-mask etched stainless steel manufactured components. (a) a blade for removing sutures with an inside radius of 200 microns, (b) etched and partially etched hard disk drive suspension load beam before forming operations where the pockets are for adhesive retention, and (c) comparison of ground (left) and etched (right) surgical blades. SEM images to same scale.

Experimental Cell Design

Initial attempts at EIS measurements were performed on a disk-shaped exposed coupon (304 stainless steel) and yielded results that were difficult to interpret. Huang, *et al.*, published (in 2007) a series of papers on the influence of current and potential distributions on a disk electrode.^{1,3} They provided a definition for dimensionless frequencies that would arise when different electrode physics were in play. For a system acting as an ideal capacitor or as a faradaic reaction without time-constant dispersion, they reported that frequency dispersion caused by electrode geometry was not seen at frequencies such that^{1,2}

$$K = \frac{2\pi f C_0 r_0}{\kappa} < 1 \quad (1)$$

where f is the frequency in Hz, κ is the electrolyte conductivity in S/cm, r_0 is the radius of the sample disk, and C_0 is the capacitance

in F/cm². For a system showing Constant-Phase-Element (CPE) behavior, the corresponding condition was reported to be³

$$K = \frac{(2\pi f)^\alpha Q r_0}{k} < 1 \quad (2)$$

where Q is a CPE parameter with units of F/s^(1- α)cm², k is the electrolyte conductivity in S/cm, and α is the CPE exponent. To maximize the frequencies usable to characterize the electrode processes, the disk size was minimized and the electrolyte conductivity was increased as much as possible.

To illustrate the effect of the influence of the current and potential distribution on the attainable frequencies, experimental data were collected for disks of 8.0 mm diameter and 3.2 mm diameter. The disk size was controlled by using a punched mask applied over the steel coupon. Impedance scans were obtained at the open circuit potential with a 10 mV amplitude in a neutral pH sodium borate buffer solution with a conductivity of about 9 mS/cm. After regressing the data to a CPE, there was a distinct lack of fit seen in the residual error and in the phase angle (Fig. 2). These points occur for frequencies $K \geq 1$, which corresponds to a frequency of about 200 Hz for a disk size

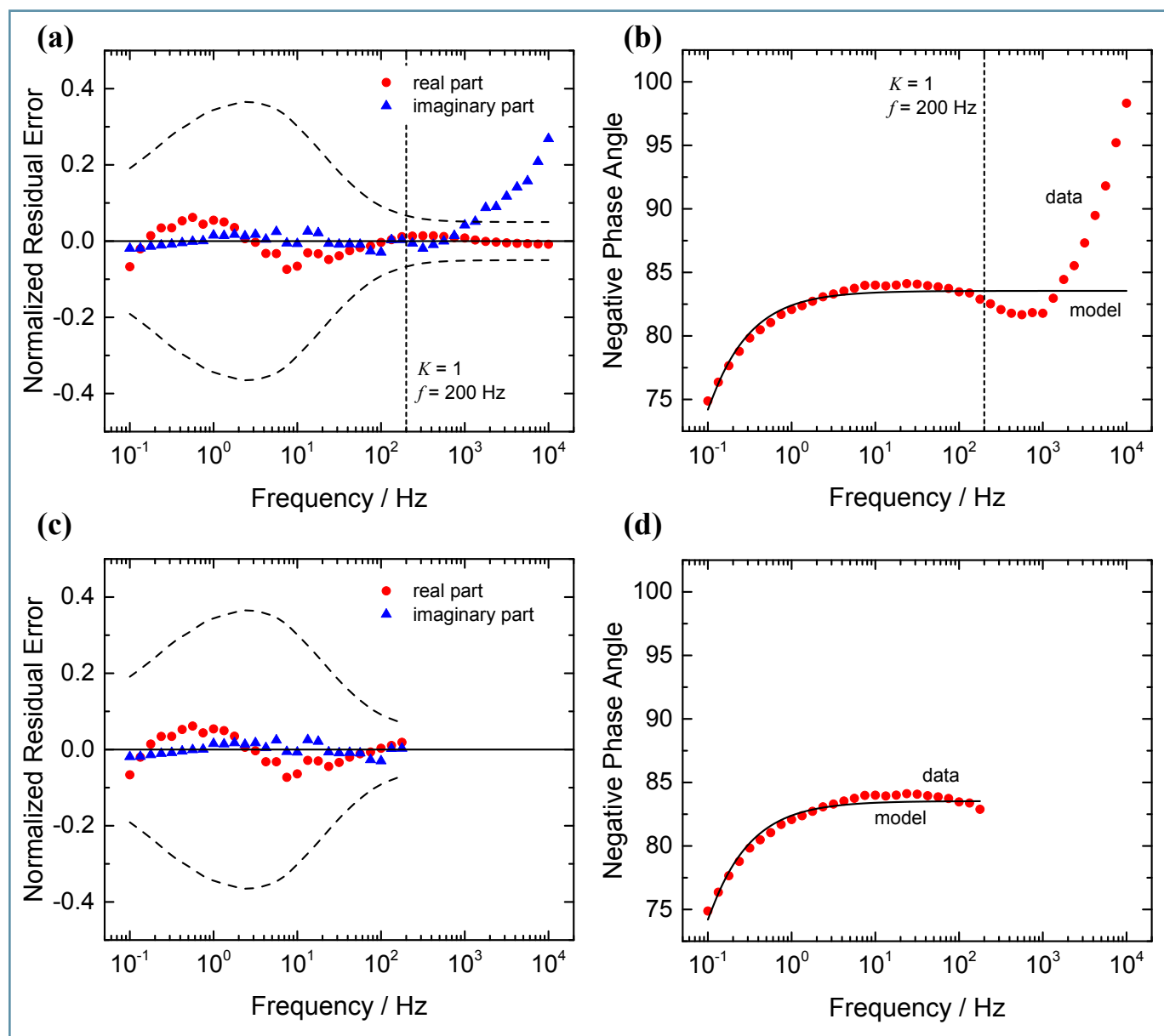


FIG. 2. Residuals and phase angle for data obtained on an 8 mm diameter disk of 304 stainless steel. (a) and (b) show significant discrepancy from a regression to a CPE in the high frequency range of the data. (c) and (d) show the fits after removing data points that are influenced by a non-uniform current and potential distribution using Eq. 2.

of 8 mm. Figure 2c and d show the same data set regressed without the data points where $K \geq 1$. The quality of fit is significantly better. However, the value for the solution resistance is off by 30%, probably due to the low maximum frequency usable.

Equation 2 indicates it may be possible to increase accessible frequencies by decreasing the disk size for the sample. For a disk size of 3.2 mm diameter and the same electrolyte, Eq. 2 indicates that frequencies up to 1500 Hz are usable. Figure 3 shows the residuals and phase angle similar to Fig. 2, but for a 3.2 mm diameter disk. Once again, when data points where $K \geq 1$ are removed from the model fit, the quality of fit to the CPE model is much improved. Also, the solution resistance obtained from regressed parameter (R_e) is 184 Ω , which is within 5% of the theoretical value of 175 Ω .

Interpretation of Impedance Results

The data obtained above at frequencies below $K=1$, such that current and potential distributions did not contribute to frequency dispersion, was best fit by a single constant-phase element. However,

the meaning of the parameters was unclear. In principle, the oxide film thickness on the surface of the disk should be obtained from

$$C = \frac{\epsilon\epsilon_0}{\delta} \quad (3)$$

where C is the capacitance δ is the film thickness, and ϵ is the film dielectric constant. The dielectric constant for oxides on steel is available from the literature, and the thickness obtained from Eq. 3 could be compared to ex-situ values obtained by XPS. The XPS depth profile obtained for the same material sample is shown in Fig. 4. Analysis of the oxygen profile indicates that the oxide is approximately 2.0 nm thick.

The problem faced herein is that the CPE model provides parameters Q and α , not capacitance. None of the models published before 2010 that yielded a value of capacitance from CPE parameters gave reasonable values for the oxide thickness.

When examining the fit parameter Q , and comparing ratios of Q resulting from material lots that behaved differently during processing (say, due to loss of resist adhesion) it was found that the ratio of the

(continued on next page)

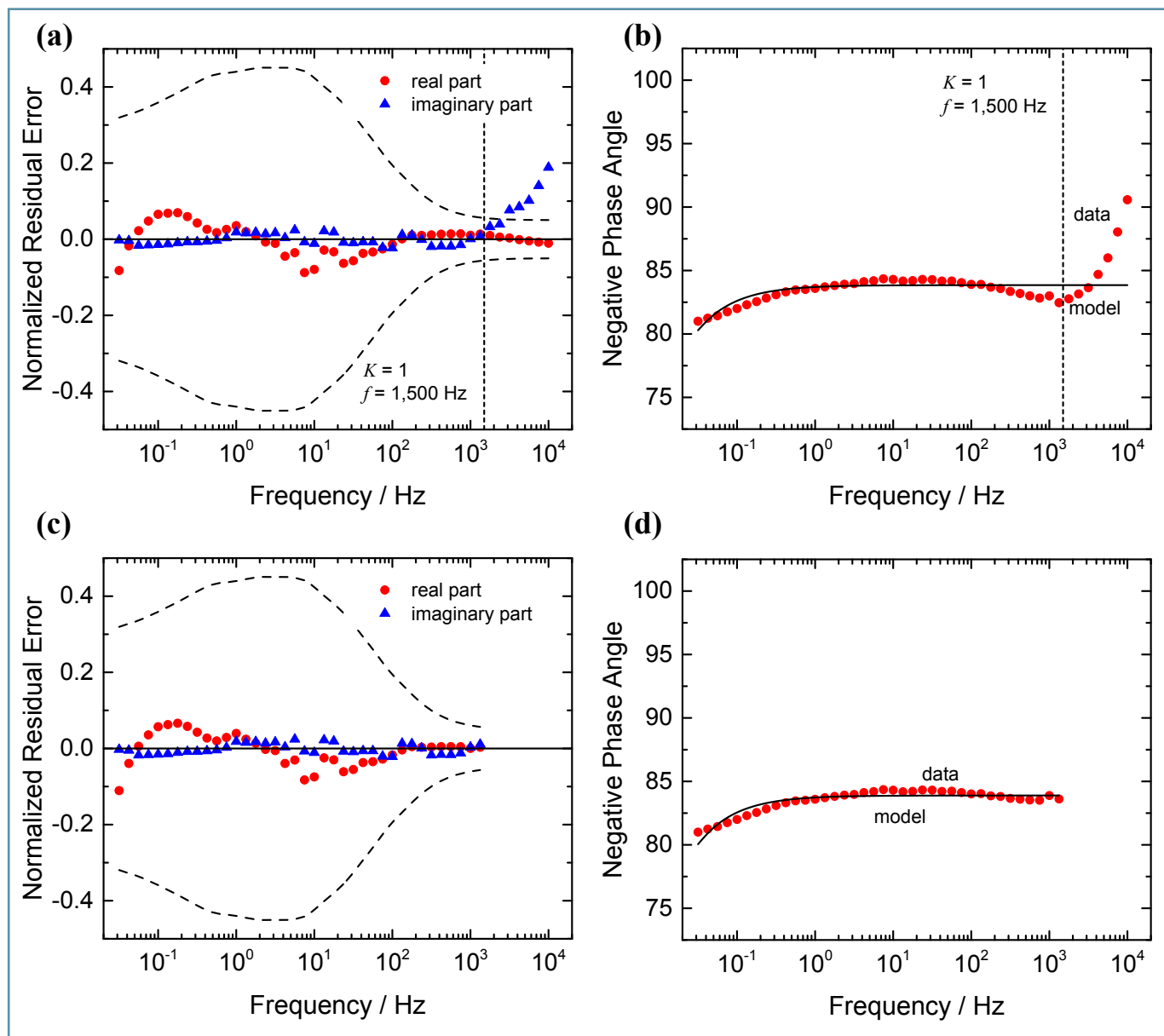


FIG. 3. Residuals and phase angle for data obtained on a 3.2 mm diameter disk of 304 stainless steel. (a) and (b) show significant discrepancy from a regression to a CPE in the high frequency range of the data. (c) and (d) show the fits after removing data points that are influenced by a non-uniform current and potential distribution using Eq. 2.

oxide thickness matched the inverse ratio of the parameter Q from the impedance model fit. It was therefore assumed that the CPE was representative of the oxide thickness.

In 2010, Hirschorn, *et al.*, published a paper in which a distribution of resistivity through the depth of the film was assumed to yield CPE behavior.^{4,5} They found a relationship among the CPE parameters and film properties as

$$Q = \frac{(\epsilon\epsilon_0)^\alpha}{g\delta\rho_\delta^{1-\alpha}} \quad (4)$$

where

$$g = 1 + 2.88(1-\alpha)^{2.375} \quad (5)$$

is a known function of α , resistivity ρ_δ is the lower bound for the resistivity distribution. Under the assumptions that for two measurements labeled 1 and 2, film properties ϵ and ρ_δ may be assumed equal and $\alpha_1 = \alpha_2$,⁶ we get:

$$\frac{Q_2}{Q_1} = \frac{\delta_1}{\delta_2} \quad (6)$$

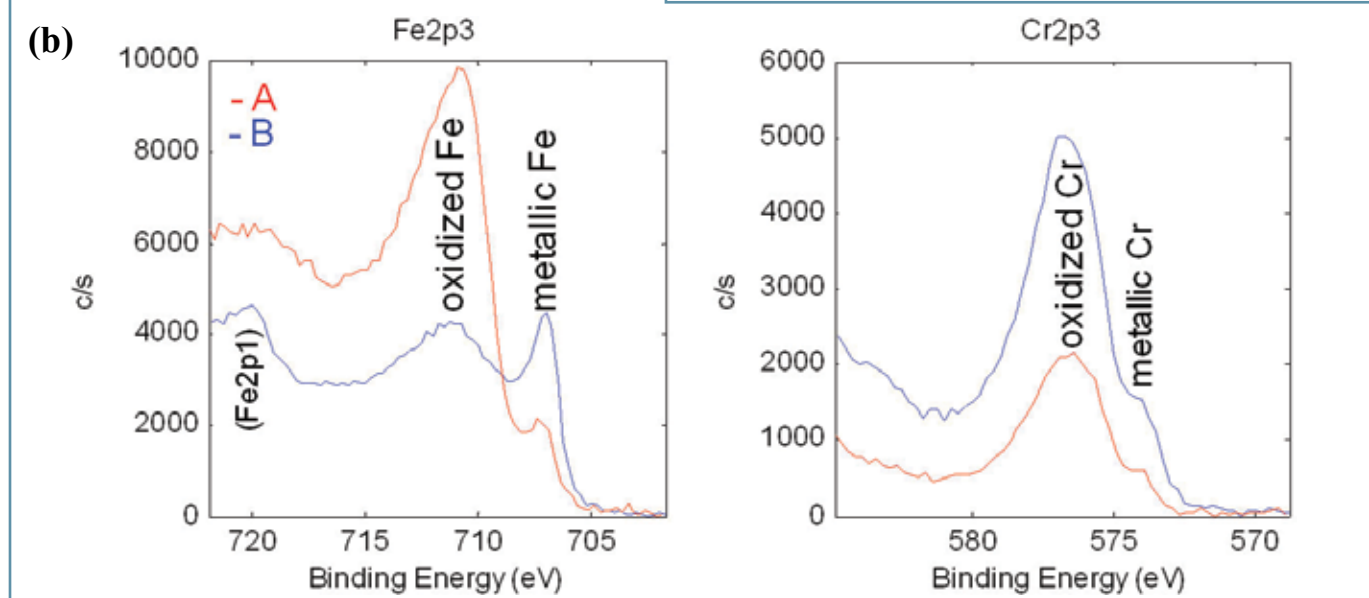
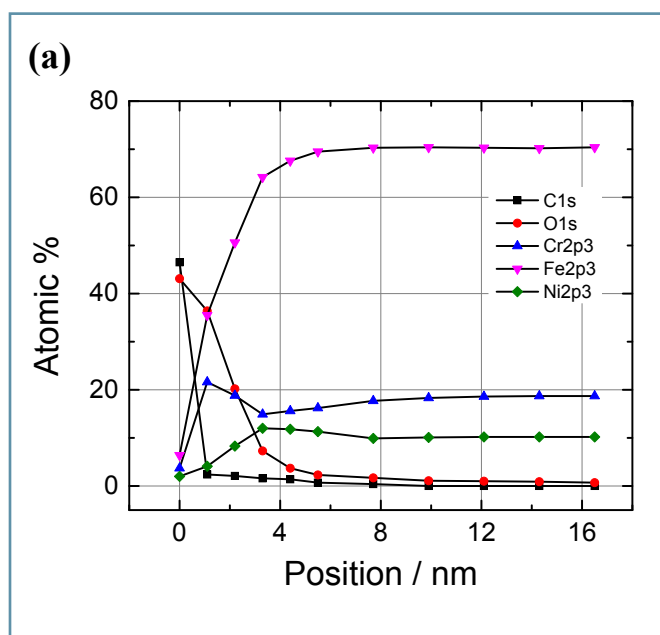


FIG. 4. (a) XPS depth profile for the model 304 stainless steel sample (studied by EIS, above) and (b) XPS survey analysis of high performance (-B, blue line) and low performance (-A, red line) stainless steel components (from example discussed below).

which is in agreement with experimental observations. Quantitative values for film thickness can be obtained from Eq. 4. Details are provided in reference [7]. For the example data shown above, the value of the oxide thickness from Eq. 4 is 1.7 nm, assuming the literature supplied value for $\rho_\delta = 450 \Omega \cdot \text{cm}$. This is in excellent agreement with the XPS data (which yielded a value of 2 nm).

This is an important development because it demonstrates that oxide film thickness can be determined directly from an inexpensive and rapid electrochemical measurement as opposed to an intrusive and time-consuming method such as XPS.

Discussion

Interpretation of electrochemical measurements such as EIS data, CV scans, pulse voltammetry, etc. requires a basic understanding of the mathematics of the underlying processes. Utilization of this fundamental knowledge can be used to improve experimental techniques to obtain truly useful information. In our case, the elimination of the contribution of non-uniform current distributions to the CPE behavior of an oxide film on a stainless steel disk electrode was important to extracting oxide characteristics. This came about through the use of local impedance measurements to see their impact on the global impedance. Most of us do not have the ability to make the types of measurements described,¹⁻⁴ but the examples and references cited here clearly show how to make measurements without undue influence of additional phenomena unrelated to the quantities of interest. In this case study, once the measurements methods were improved, one could tackle the more interesting work of interpreting the physical meaning of the CPE. It was immediately apparent that ratios of the regressed parameter Q were inversely proportional to the ratios of oxide thickness obtained by XPS (Eq. 6). In this way, collaboration between the authors of this paper and others was initiated where the models being developed and published^{4,5} were tested and verified under real manufacturing conditions.^{6,7}

As an example, a problem was encountered during manufacturing wherein resistance welding of a copper component to a stainless steel component yielded an interface with variable peel strength. Analysis of high and poor performance steel components by EIS revealed that the poorly performing steel had an oxide thickness of 4.4 nm, but the high performance parts had an oxide thickness of 2.7 nm. XPS survey analysis (Fig 4b, no depth profile performed) confirmed a thinner oxide on the high performance steel by way of a strong metallic iron and chrome presence in the scan, but the poor performing metal showed almost no metallic iron or chrome signal. Given the escape

depth of photoelectrons for XPS on the machine used was about 50 Å, the lack of a metallic iron or chrome signal is in line with the EIS determined oxide thickness of 4.4 nm. An additional interesting piece of information from the XPS data was that the chrome to iron ratio of the high-performance (thin oxide layer) sample was four times that of the poorly performing (thick oxide layer) sample, which seems to not interfere with the oxide thickness measurement. This may be attributed to the fact that both the iron oxides and chrome oxides share a similar dielectric constant assumed to be 12.

Impact on Industrial Processes

The impedance based screening of raw materials has a tremendous positive impact in an industry where the state of the oxide film on stainless steel strongly influences process and product performance. Having a fast, inexpensive and accurate measure of the film thickness is of great benefit in the manufacturing process. With such a technique, process excursions such as a small air leak in an annealing furnace can be diagnosed and remedied within hours, thereby preventing large amounts of product loss and possible shipping delays.

Process development can be improved because of improved knowledge of how constitutive processes alter the oxide on stainless steel or how they depend on its state. Knowing that a new component to be manufactured has incompatible adjacent process steps with regard to the oxide state can save a great deal of time and effort in debugging the manufacturing steps.

Furthermore, incoming raw materials can be screened rapidly to determine what type of cleaning/pre-processing is necessary and sufficient. This also can avoid processing problems during downstream processing.

Conclusion

In the last several years, significant progress has been made in the understanding of EIS data obtained on stainless steels. The work of Huang, *et al.*,¹⁻³ made clear many of the shortcomings inherent in the experimental methods used to obtain EIS data. While geometrically induced current and potential distributions on a disk electrode in themselves are an interesting phenomenon, they are a distraction from measuring a useful property (thickness) of the oxide films formed on metal surfaces. Understanding what parts of the impedance spectra are truly useful requires an inherent understanding of the fundamental mathematics, and leads to the ability to make accurate and rapid measurements of oxide film thickness by EIS. This ability is invaluable from a manufacturing perspective as it serves as a method to screen the incoming raw material, as well as the product in-between different steps in the manufacturing process, allowing for greatly enhanced quality control. ■

About the Authors



DOUGLAS RIEMER has been a Staff Scientist at Hutchinson Technology, Inc. of Minnesota for the last eight years. He works in the Advanced Materials and Process Development group, and holds 8 patents and trade secrets covering inventions in electro and electroless plating, etching, polishing and materials surface characterization. He graduated in 2000 from the University of Florida with a PhD in Chemical Engineering. He is currently the vice-chair of the Industrial Electrochemistry & Electrochemical Engineering Division (IE&EE) of ECS. He can be reached at riemerdp@hotmail.com.



MARK ORAZEM, Professor of Chemical Engineering at the University of Florida, is a Fellow of The Electrochemical Society and is the Immediate Past President of the International Society of Electrochemistry. He served for 10 years as Associate Editor for the *Journal of the Electrochemical Society* and co-authored, with Bernard Tribollet of the CNRS in Paris, a textbook entitled *Electrochemical Impedance Spectroscopy*. In 2012, Prof. Orazem received the Henry B. Linford Award of the Electrochemical Society, and, in 2014, he was named a University of Florida Research Foundation professor. He currently chairs the Education Committee for the ECS and regularly offers short courses on impedance spectroscopy at ECS meetings. He can be reached at meo@che.ufl.edu.

References

1. V. Huang, V. Vivier, M. Orazem, N. Pébère, and B. Tribollet, *J. Electrochem. Soc.*, **154**, C99 (2007).
2. V. Huang, V. Vivier, M. Orazem, N. Pébère, and B. Tribollet, *J. Electrochem. Soc.*, **154**, C81 (2007).
3. V. Huang, V. Vivier, M. Orazem, I. Frateur, and B. Tribollet, *J. Electrochem. Soc.*, **154**, C89 (2007).
4. B. Hirschorn, M. E. Orazem, B. Tribollet, V. Vivier, I. Frateur, and M. Musiani, *J. Electrochem. Soc.*, **157**, C452 (2010).
5. B. Hirschorn, M. E. Orazem, B. Tribollet, V. Vivier, I. Frateur, and M. Musiani, *J. Electrochem. Soc.*, **157**, C458 (2010).
6. M. E. Orazem, B. Tribollet, V. Vivier, D. P. Riemer, E. A. White, and A. L. Bunge, *J. Braz. Chem. Soc.*, **25**, 532 (2014).
7. M. E. Orazem, B. Tribollet, V. Vivier, S. Marcelin, N. Pébère, A. L. Bunge, E. A. White, D. P. Riemer, I. Frateur, and M. Musiani, *J. Electrochem. Soc.*, **160**, C215 (2013).